R-11-18

Interaction of clay and concrete plugs – Plugging of 5 m deep hole KA1621G01 at Äspö

Final report

Roland Pusch, Drawrite AB, Luleå Technical University

Gunnar Ramqvist, Eltekno AB

November 2011

Svensk Kärnbränslehantering AB
Swedish Nuclear Fuel
and Waste Management Co

Box 250, SE-101 24 Stockholm
Phone +46 8 459 84 00

ISSN 1402-3091
SKB R-11-18
ID 1240445

Interaction of clay and concrete plugs – Plugging of 5 m deep hole KA1621G01 at Äspö

Final report

Roland Pusch, Drawrite AB, Luleå Technical University

Gunnar Ramqvist, Eltekno AB

November 2011

Summary

Sealing of deep boreholes in repository rock is planned to be made by installing dense smectite clay plugs where the rock is low-permeable and casting concrete where the holes intersect water-bearing fracture zones. Such zones have to be stabilized before sealing starts because fragments of rock can otherwise fall off and make it difficult to bring equipment for concrete casting and clay plug units down. These parts of the holes are filled with concrete and clay plugs are then inserted up to the nearest fracture zone where concrete is filled to the required level etc. The role of the concrete in the hole and in the closest part of the surrounding fracture zone is to provide stable parts that are sufficiently fine-porous to prevent clay particles from contacting clay plugs to migrate into the fractures and be lost by erosion.

While the larger parts of long clay plugs are believed to stay largely intact chemically for hundreds of thousands of years, the parts adjacent to concrete plugs may undergo changes and so can the concrete plugs themselves. The objective of the presently reported project was to identify the detailed processes and quantify associated changes in physical properties by investigating samples of clay and concrete from a 2.5 m long plug of clay over which an equally long concrete plug had been cast and left to rest for 3 years.

The outcome of the investigations was that significant chemically induced changes in mineralogy and physical performance had occurred within a few centimetres distance from the clay/concrete contact but that virtually no changes had taken place at larger distance. A comprehensive laboratory study including X-ray diffraction (XRD), X-ray fluorescence (XRF) and electron microscopy study (SEM and TEM) on the sample material was performed including also dual beam (combined ion and electron) microscopy. It was found that the clay had infiltrated the contacting concrete plug after filling of the borehole since clay was detected both along the contact between the plug and the borehole wall as well as interleaved within the bottom of the concrete fill.

Chemical alteration of the cement mineral phases at the clay-concrete contact released some quantities of Ca and K that had partly replaced Na in the interlayer of the clay. Precipitation of gypsum and halite had occurred as well as chemical modifications of the clay. The cement has clearly been altered in contact with the clay plug and has lost part of the material strength. Neocrystallization of a fibrous Ca-Si phase had occurred along with the formation of some amorphous components. Dissolution in the saline water is the probable mechanism.

The major practical consequence of the chemical interaction of contacting clay and concrete is that the clay becomes slightly less expandable and slightly more conductive within a few centimetres distance from the contact and that the concrete loses some of its strength in 3 years. The adhesion between concrete and rock appeared to be low and concrete plug segments could easily be extruded from the discs by hand.

Sammanfattning

Försegling av djupa borrhål i förvarsberget görs lämpligen genom att placera in lerblock med hög densitet där berget har låg genomsläpplighet och gjuta betong där hålen går igenom vattenförande sprickzoner. Sådana zoner måste stabiliseras innan förseglingen kan börja eftersom bergfragment annars kan falla ned och omöjliggöra införandet av utrustningar och pluggkomponenter. Dessa delar fylls sedan med betong och härefter med lerpluggar till nästa sprickzon osv. Den avsedda funktionen hos betongen i hålet och den omgivande sprickzonen är att åstadkomma en stabil pluggdel som hindrar att partiklar från den närmaste lerpluggen vandrar in i bergsprickorna och förs bort genom erosion.

Medan den övervägande delen av lerpluggarna antas förbli intakt i hundratusentals år kan de delar som är i kontakt med betongpluggar ändras liksom pluggarna själva. Problemet är att identifiera nedbrytningsprocesserna och bestämma hur långt från kontakten mellan dessa komponenter som de når. Det här rapporterade projektet syftade till att i detalj identifiera processerna och kvantifiera orsakade förändringar i fysikaliska egenskaper genom undersökning av prover tagna från ett borrhål med en 2.5 m lång lerplugg över vilken en lika lång betongplugg hade gjutits och vilat i tre år.

Den viktigaste erfarenheten från undersökningen var att betydande kemiskt betingade förändringar av mineralinnehållet och de fysikaliska egenskaperna hade skett inom några få centimeters avstånd från kontakten mellan lera och betong medan förändringar på större avstånd inte kunde ses. En omfattande laboratorieundersökning omfattade röntgendiffraktion (XRD), röntgenfluorescens (XRF) och elektronmikroskopi (SEM and TEM) med kombinerad jon- och elektronmikroskopi gjordes. Det befanns att lera hade infiltrerat anslutande betong eftersom lera fanns i kontakten mellan betong och borrhålsvägg och också bildat skikt i betongen.

Kemisk förändring av cementmineralfaserna i kontakten med leran orsakades av frigörandet av små mängder av Ca och K som delvis ersatte Na i leran. Utfällning av gips och natriumklorid hade skett och kemisk ändring av lermaterialet hade inträffat. Cementmaterialet i kontakt med leran hade fått sin hållfasthet minskad. Det hade ändrats vid kontakten med leran genom jonbyte och nykristallisation av en fibrös Ca-Si fas samtidigt med bildning av en amorf komponent. Lösning i det salta grundvatten är den sannolika mekanismen.

Den viktigaste praktiska följden av den kemiska samverkan hos lera och betong i kontakt är att leran på tre års tid blir något mindre svällande och något mer konduktiv inom några centimeters avstånd från kontakten, och att betongens hållfasthet minskar. Om degraderingen sker genom diffusiva processer kan man anta att leran förändras påtagligt till någon meters avstånd från kontakten på 500 år och till två meters avstånd på 3000 år medan betongen undergår mindre ändring. Efter detta har ytterligare förändringar av leran knappast skett. Eftersom cementkomponenten är den drivande kraften rekommenderas framtagning av en mindre aggressiv betongsort. Det skulle lösa problemet med inpressning av lera i betongen om viskositeten höjs och härdningen kan ske snabbare. Användning av oorganiskt flytmedel skulle sannolikt förbättra adhesionen till borrhålsväggarna.

Contents

1 Objective

The report describes the outcome of the work within the sub-project 4 "**Interaction of clay and concrete plugs"** within phase 4 of the project **"Sealing of investigation Boreholes"** TU 02.

Sealing of deep boreholes in repository rock is planned to be made by installing dense smectite clay plugs where the rock is low-permeable and casting concrete where the holes intersect water-bearing fracture zones (Pusch and Ramqvist 2004). The parts of a hole passing through such zones shall be filled with a mixture of suitably graded quartz material stabilized by a small amount of low pH cement[1] (Q/C plug). While the larger parts of long clay plugs are believed to stay nearly intact chemically for hundreds of thousands of years, the parts adjacent to the concrete plugs may undergo changes and so can the concrete plugs themselves. The objective of the presently reported project was to identify the detailed processes and quantify associated changes in physical properties by investigating samples of clay and concrete from a 2.5 m long plug of clay over which an equally long concrete plug had been cast and left to rest for 3 years.

The problem is to find out what the degradation process is and how far from the contact of the two components that it extends. The latter would require that the test be conducted for a very long time but once the process has been identified it should be possible to derive a theoretical model that can be used for predicting the extent of the degradation over the operational period of a repository for High-level waste. The purpose of the present experiment with Q/C plugged holes bored from a tunnel at 220 m depth was to get a basis for working out conceptual and theoretical models for long-term performance of such plugs. The design principle is shown in Figure 1-1.

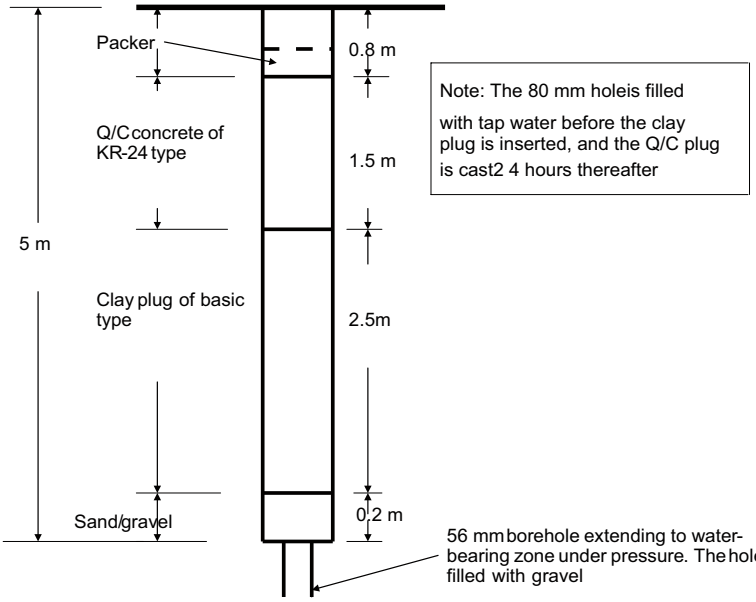

Figure 1-1. *Schematic view of the two 5 m boreholes (actual depths 6.00 and 5.90 m) with 80 mm diameter for testing of the interaction of quartz/cement and clay. The upper end of the hole is sealed by a mechanical packer equipped with a manometer and a valve for recording and controlling the water pressure in the central copper pipe that extends down into the sand/gravel fill. The clay plug is of "Basic" type.*

[1] The use of low pH cement is for minimizing chemical reactions between concrete and smectite.

2 Conditions on site

2.1 General

The conditions for investigating chemically induced changes of clay and contacting cement-stabilized quartz concrete partly depends on the confining rock, which is illustrated in Figure 2-1. The ground water at the investigation site is brackish which would cause dispersion and settlement of clay exfoliated from the dense clay core, which could disturb the maturation of the clay. The hole was therefore filled with low-electrolyte water before placing the plugs. With time, electrolytes diffuse from the groundwater in the rock into the clay causing changes in physical performance that are stronger where the water is rich in salt than where the salt concentration is low. The access to water is the most important factor for maturation of the clay. It is controlled by the rock structure and water pressure.

Extracting the plugs by overcoring after different periods of time makes it possible to identify changes in physical properties and chemical composition.

2.2 Rock structure

The structural constitution of the rock mass in which the holes were bored has not been modelled but some general features can be imagined by use of core photographs. The photo in Figure 2-1 illustrates the rather low frequency of intersected fractures.

Core examination indicated that the average distance between water-bearing fractures that are intersected by the holes is 1 m in the depth interval 2.3 to 5 m, i.e. where the clay plugs were located.

2.3 Hydrology

Inflow measurements soon after the boring had been made indicating that the small inflow would retard the maturation of the plugs and the holes were therefore extended down to about 20 m depth below the floor by percussion drilling of 35 mm diameter holes. The inflow was still not significant, indicating that rather few water-bearing fractures below 5 m depth had been intersected and also that the two holes are hydraulically interacting through subhorizontal or slightly inclined fractures. Inflow and pressure measurements in mid October 2006 showed that one of the holes, KA1621G01 had an insignificant water inflow and that the other, KA1621G02 was even “drier”, suggesting slow maturation and chemical interaction of the plugs in the latter hole. The water pressure in the rock surrounding the holes has been estimated to be about 1 MPa.

Figure 2-1. *Hole KA 1621 G02. The core from the 80 mm-diameter hole represents the uppermost 3 meters of the hole having at least five water-bearing fractures.*

3 Test arrangement

3.1 Bottom fill

The plugs were installed in October/November 2006. The holes were filled with medium-coarse sand to about 5 m from the floor for providing water from the deeper parts to the plugs (cf. Figure 1-1). The sand was poured in the holes and compacted with a rod. The dry density of the fill was estimated to be about 1,000 kg/m^3 and the void size in the range of 10 to 500 μm, which would allow some but not significant migration of particles from the adjacent clay plug into it.

3.2 Clay plugs

The clay plug in the 80 mm diameter holes was of "Basic" type (Pusch and Ramqvist 2004) and had the following data:

- Outer and inner diameters of the copper tube with 50% degree of perforation were 76.1 and 72.1 mm, respectively. The length was 2.5 m.
- The clay blocks, which were trimmed to fit tightly in the tubes, had 6% water content and a density of 2,150 kg/m^3, corresponding to a dry density of 2,028 kg/m^3. The void ratio and initial degree of saturation were e=0.37 (porosity 0.27) and 45%, respectively. The predicted ultimate density of the plugs after complete water saturation was 2,078 kg/m^3.
- The borehole was filled with tap water before inserting the clay plug.

3.3 Concrete plugs

The concrete plugs were made of concrete developed by CBI[2] (Table 3-1) cast directly on the clay plug 8 hours after placing this plug. This made it mature sufficiently much to prevent the semifluid concrete to enter the gap between the copper tube and the rock and displace the clay "skin" formed around the copper tube in the clay plug. The outcome of the test showed that this goal was not reached as described in Section 6.3.1.

Table 3-1. Concrete (low strength) recipe for plugging of boreholes.

Components	Amount (kg/m^3 concrete)	Manufacturer
White cement	60.0	Aalborg Portland
Silica Fume	60.0	Elkem
Fine-ground α-quartz M300	200.0	Sibelco
Fine-ground cristobalite M6000	150.0	Sibelco
Superplasticizer Glenium 51	4.375 (dry content)	Degussa
Granitic aggregates 0–4 mm	1,700.0	Jehanders grus
Water	244.27	local

[2] Cement och Betong Institutet (Lagerblad B. & Vogt C., 2004).

4 Prediction of hydration and maturation

4.1 Scope

The access to and composition of water entering the Q/C plug determine the rate of maturation and consistency of both the clay and concrete components. These factors were assessed in the study and taken as a basis for the planned conceptual models.

4.2 Concrete plugs

The water pressure was low in the rock and saturation and maturation of the plug components were expected to be slower than in rock with unlimited access to water. Still, it was estimated that all major chemical processes would have proceeded far enough for making relevant chemical analyses.

For hydration and maturation of the concrete plug enough water is assumed to have been provided by the surrounding rock and the majority of all the mineralogical processes are assumed to have taken place within one year. Theoretical considerations and studies using batch tests have indicated that ordinary Portland cement can give unwanted reaction products in the clay in a few months (Pusch et al. 2003). For low-pH cement considerably less impact on the clay is expected.

4.3 Clay plugs

The fact that the hole will be filled with tap water before the plugs are inserted would imply that the initial phase of formation of a clay "skin" takes place within less than a day (Pusch and Ramqvist 2004). The expected low density of this skin may make early chemical interaction with cement water possible to a significant distance from the contacts between the plugs. Dissolved elements and water migrate from the fresh cement paste to the smectite in the first few hours. Ca migrates from the cement to the clay causing ion exchange and change in the microstructure of the clay by coagulating softer parts. This was planned to be documented by microstructural (SEM and TEM) analyses and determination of the hydraulic conductivity and swelling pressure of clay samples at different distances from the clay/concrete contact.

The subsequent maturation of the clay plugs was concluded to be predictable by applying the same simple model as used for foreseeing the fate of clay plugs as described in Sub-projects 1 and 2 of Phase 3 (Pusch and Ramqvist 2007). This is because the constitution of the rock and prevailing water pressure were found to be relevant for a fairly short study of the interaction of concrete and smectite clay.

5 Program for evaluation of the evolution and conditions of the plugs

5.1 Principle

The determination of key properties of the extracted plugs of clay and concrete was followed the standard SICADA data base procedure. Four major properties were determined and reported:

1. Hydraulic conductivity and expandability.
2. Rheology.
3. Mineralogy.
4. Chemistry.

1. Hydraulic conductivity and expandability

Oedometer tests of trimmed clay and concrete samples are made, the latter tests requiring that the samples are coated with thick smectite paste for avoiding leakage along the steel/concrete contact. This gives hydraulic conductivity data, the tests being performed with hydraulic gradients up to 50.

2. Rheology

For clay samples oedometer testing is employed for determining the swelling pressure. For concrete samples unconfined compression tests are used.

3. Mineralogy – XRD

XRD analysis of packed and sedimented samples is made of clay and concrete taken at different distances from the contact. SEM and TEM electron microscopy are conducted for characterizing of the microstructure of virgin materials and samples in the plugs.

4. Chemistry – Element concentration

Chemical analyses are performed of virgin materials and samples in the plugs with respect to the element distribution (EDX, XRF).

5.2 Investigation of recovered borehole seals

5.2.1 Objective

The purpose of the project was to investigate if smectitic clay plugs interact chemically with contacting concrete of CBI-type to a practically important extent. The plugs had been in the holes for 3 years but changes were expected to be small. A second neighbouring hole of the same type can be investigated later (cf. “Objective”).

5.2.2 Preparation of samples

The plugged borehole was recovered from the rock by slot-drilling to give a rock column of about 6 m length in late November 2009 (Figure 5-1). The activity is described in activity plan AT TD TU02-09-069. It was stored in a shed at a temperature of about 5ºC until mid January 2010 when it was sectioned by wire-sawing. The most important part was the contact of clay and concrete but samples at various distances where also taken and samples were also extracted and saved for reference purposes (Figure 5-2). Figure 5-3 illustrates sections obtained by wire sawing. Samples for geotechnical and chemical analyses were stored at 5ºC in the laboratory before being tested at SWECO’s lab and at the geological laboratory of Greifswald University in January/February 2010. The slot drilling procedure is described in detail in Appendix B.

Figure 5-1. *The rock column containing the plugged borehole KA 1621 G02. Upper: Slot drilling. Lower: Wire sawing of discs with about 100 mm thickness.*

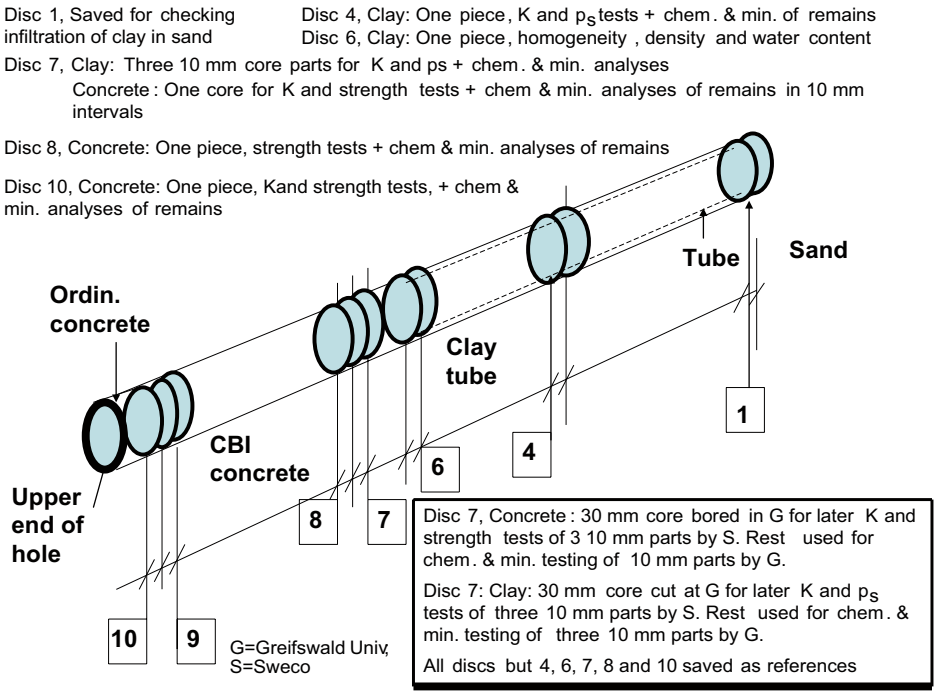

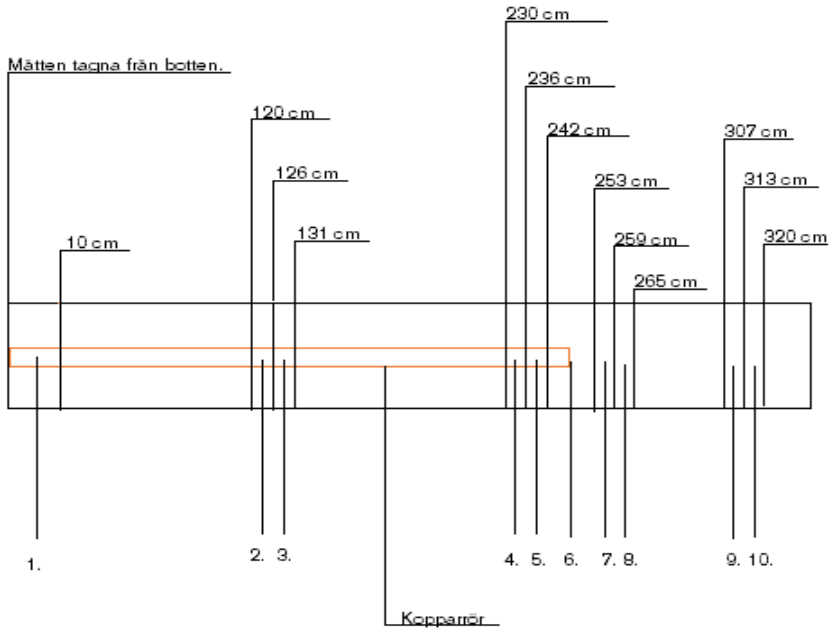

Figure 5-2. *Sectioning for obtaining discs of the sealings. Upper: Principle. Lower: Exact positions of sections and discs.*

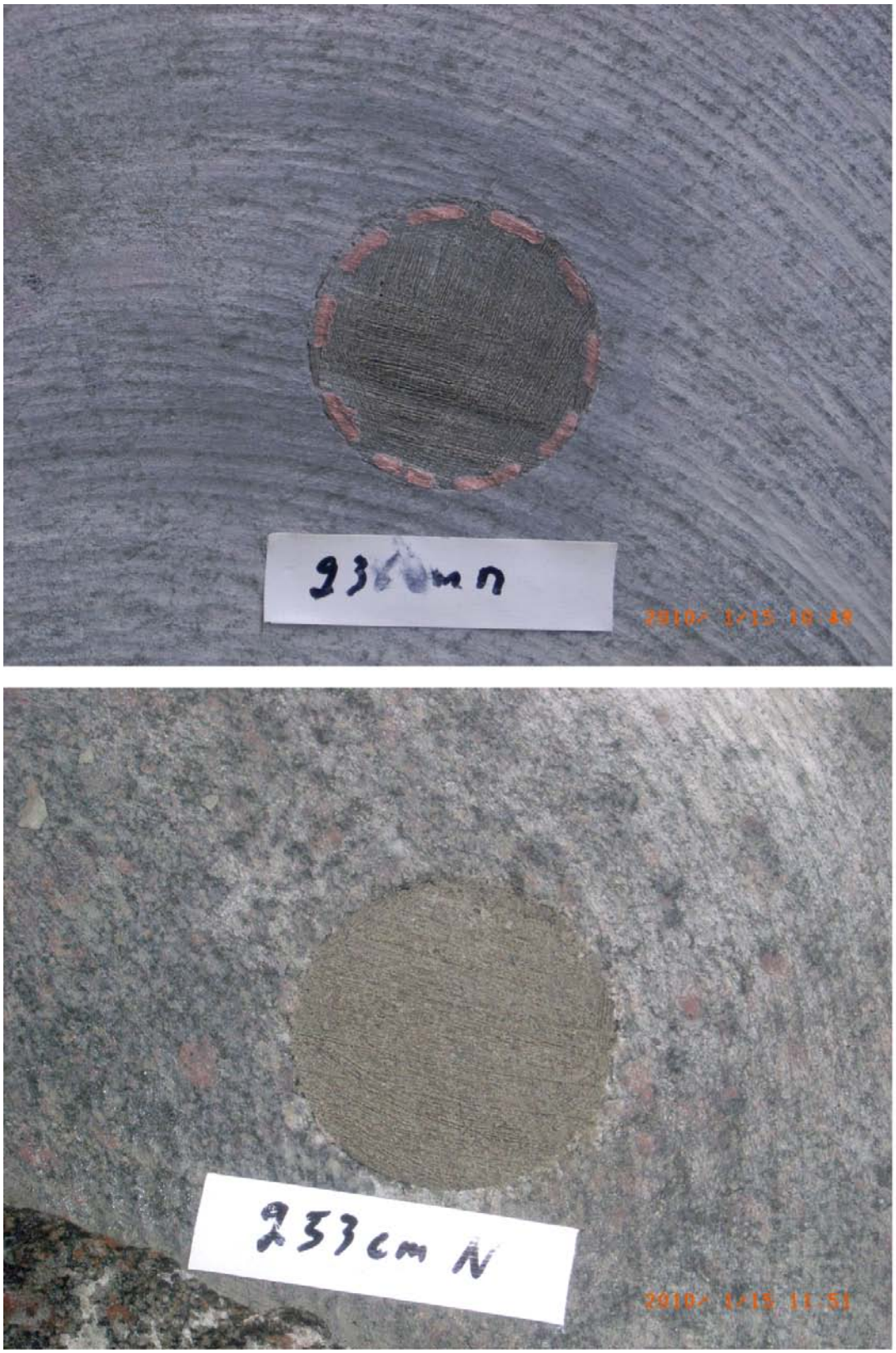

Figure 5-3. *Examples of sections. Upper: Clay plug (base of Disc 5). Lower: The CBI-concrete seal (base of Disc 7). Both the clay and the concrete had completely filled the hole.*

5.3 Final laboratory program

5.3.1 Concrete

Samples of concrete ("cores") with 26–28 mm diameter and 40 mm length were bored from Disc 8 for measuring the hydraulic conductivity and unixial compressive strength (cf. Figure 5-2). The remaining part was used for determining the content of major chemical components: SiO_2, Al_2O_3, CaO, K_2O and Na_2O, the distribution of the calcium element being of particular importance. The "core" with 26–28 mm diameter bored from Disc 7 was divided to represent the intervals 0–10 mm, 10–20 mm, 20–30 mm and 30–40 mm from the contact with clay and tested with respect to the hydraulic conductivity and unixial compressive strength. The remaining part was used for chemical and mineralogical characterization of the same intervals as for the concrete "core". Samples representing the intervals 0–10 mm and 30–40 mm from the contact with clay were investigated with respect to the microstructural constitution via SEM/EDX.

- The total number of samples for determining the hydraulic conductivity and uniaxial compressive strength was 2 (one from the "core" of Disc 7 and one from Disc 8, both exactly 40 mm long). For Disc 8 the coring was made at Äspö while the remaining part was brought to Greifswald University for chemical and mineralogical analyses. For Disc 7 also the sample preparation was made at Greifswald.
- The total number of samples for chemical and mineralogical analyses was 5 (three from the remaining parts of Disc 7 and two from the remaining part of Disc 8 after the coring).

5.3.2 Clay

Clay samples with 30 mm diameter och 20 mm length were cut from Disc 4 and Disc 7 for determining the hydraulic conductivity and swelling pressure (cf. Figure 5-3). From Disc 7 four 10 mm long samples were prepared representing the distance intervals from the concrete contact 0–10 mm, 10–20 mm and 20–30 mm for determination of these properties (the concrete "core" was confined in an oedometer cell and transported to Sweden determination of the unconfined compressive strength). The remaining part of Disc 4 (the entire material brought to Greifswald University) and the same three intervals as for the "core" of Disc 7 were extracted from the remaining part of Disc 4 and investigated by XRD and chemical analysis with respect to the components SiO_2, Al_2O_3, CaO, K_2O och Na_2O.

- The total number of determinations of the hydraulic conductivity and swelling pressure=4 (one from Disc 4 and four from Disc 7).
- The total number of chemical and mineralogical analyses=4 (one from the remaining part of Disc 4 and three from the remains of Disc 7.

The geotechnical investigations were made by SWECO Infrastructure AB.

The chemical and mineralogical investigations were made by Dept. of Geology, Greifswald University, Greifswald, Germany, under the heading of Prof. Laurence Warr.

5.4 Results from determination of the physical properties

5.4.1 Data obtained

Disc 4

The disc contained a well fitting part of the clay plug that was investigated with respect to the water content and density of the clay that formed a central core. The central part of the clay "core" had an average water content of 26.6% and a density of 2,000 kg/m^3 (dry density 1,590 kg/m^3). The density is slightly lower than predicted (2,078 kg/m^3), which can be explained by a slightly larger borehole diameter than 80 mm or by non-perfect fitting of the clay blocks in the tube in the preparation phase, as well as some slight erosion.

Hydraulic conductivity: 2.5E-11 m/s (Dist. water).

Swelling pressure: 3.05 MPa (Dist. water).

Test data: Weight of cup 0.7 g, Weight of wet clay 12.0 g, Weight of dry clay 9.4 g, Weight of water 2.5 g.

Disc 6

This disc contained part of the clay plug that was investigated with respect to the homogeneity, water content and density of the clay that formed a "skin" between the copper tube and the rock and of the central "core". Figure 5-3 shows the appearance of the plug extracted from the rock, verifying that the "skin" completely covered the tube. The average water content of the "skin" was 38.8% and the density 1,800 kg/m^3 (dry density 1,270 kg/m^3). The central part of the clay "core" had an average water content of 37.0% and a density of 1,850 kg/m^3 (dry density 1,350 kg/m^3), (Figure 5-4).
The density was significantly lower than the predicted value 2,078 kg/m^3.

Test data:

Skin: Weight of cup 0.6 g, Weight of wet clay 23.6 g, Weight of dry clay 17.0 g, Weight of water 6.6 g.

Core: Weight of cup 0.6 g, Weight of wet clay 31.1 g, Weight of dry clay 23.3 g, Weight of water 8.4 g.

Disc 7

This disc contained concrete of CBI-type[3] in contact with a clay plug consisting of MX-80 clay confined by a perforated copper tube.

Concrete plug

The number of samples with 28 mm diameter and 10 mm height core-drilled from the contact with clay had to be reduced to two for practical purposes. They are termed B1 (0–15 mm from the contact), and B2-(13–23 mm from the contact). Material from the remaining concrete plug at the same distances from the clay contact were analysed according to the original program.

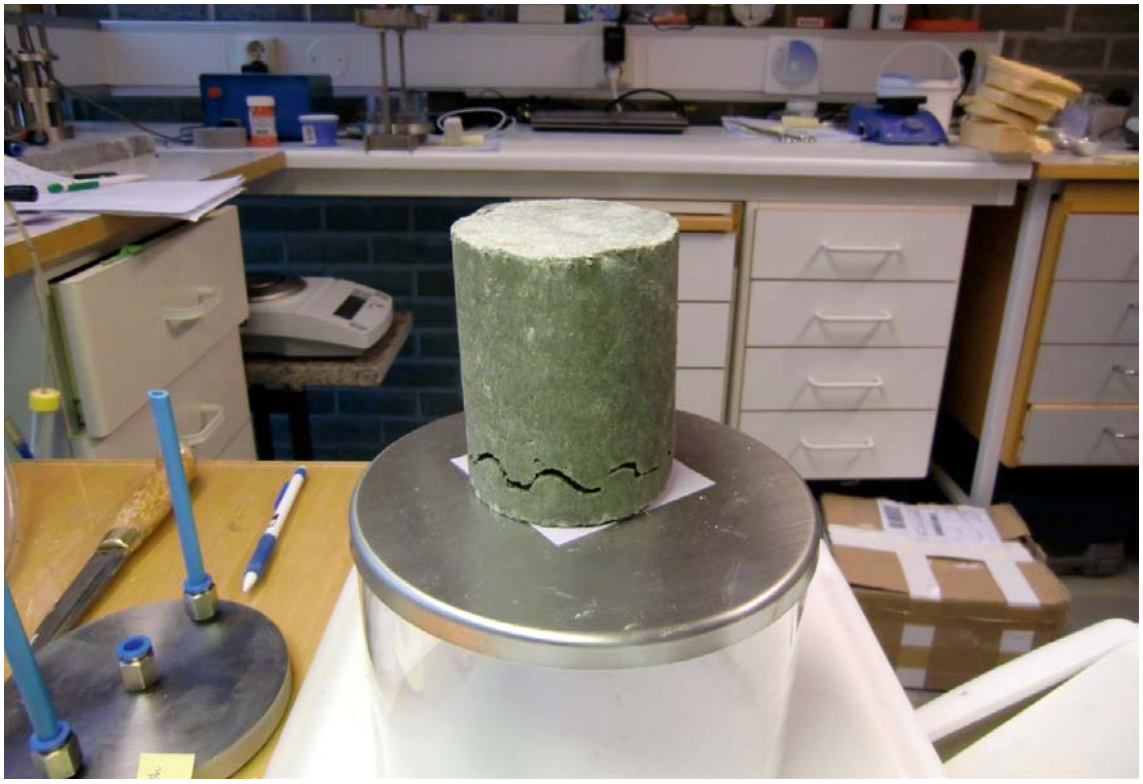

Figure 5-4. *Appearance of the clay plug released from Disc 6. The wavy fracture was caused at dissembling of the plug and occurred at the contact of a tube-confined part and one where only a clay column had been placed. This latter part is at the base of the plug but was on top of the tube-confined part in the hole.*

[3] Table 3-1.

Density,

B1=2,253 kg/m^3 (0–15 mm from clay contact).

B2=2,183 kg/m^3 (15–25 mm from clay contact).

Hydraulic conductivity

B1=3.9E-11 m/s (0–15 mm from clay contact).

B2=3.9E-11 m/s (15–25 mm from clay contact).

Compressive strength

B1=31.7 MPa.

B2=24.5 MPa.

Clay plug

Three cylindrical blocks with 30 mm diameter and 10 mm height were trimmed from the sample contacting the concrete for determining the hydraulic conductivity, swelling pressure, and compressive strength. They are termed 7L1 (0–8 mm from concrete B1), 7L2 (8–17 mm from concrete B1), and 7L3 (17–25 mm from concrete B1). Material from the remaining clay plug at the same distances from the clay contact were analysed according to the program. The density was significantly lower than the predicted value.

Density

7L1=1,800 kg/m^3 (0–8 mm from concrete B1).

7L2=1,910 kg/m^3 (8–17 mm from concrete B1).

7L3=1,880 kg/m^3 (17–25 mm from concrete B1).

Hydraulic conductivity

7L1=1.0E-11 m/s (0–8 mm from concrete B1).

7L1=2.1E-11 m/s (8–17 mm from concrete B1).

7L3=1.2E-11 m/s (17–25 mm from concrete B1).

Swelling pressure

7L1=960 kPa (0–8 mm from concrete B1).

7L2=775 kPa (8–17 mm from concrete B1).

7L3=770 kPa (17–25 mm from concrete B1).

Disc 8

This disc contained concrete that was investigated with respect to the compressive strength and hydraulic conductivity. The plug was extruded from the rock frame by axial loading, which gave

the adhesive strength of the concrete, 80 kPa. The plug was then exposed to uniaxial compression at a loading rate of about 100 kg per second leading to failure by axial splitting at almost exactly 8,000 kg. This corresponds to a compressive strength of 15.9 MPa. CBI's investigations imply that the strength would exceed 30 MPa already after a few months (CBI 2004), which indicates that chemical processes generated by the uptake of salt water from the rock, or ageing, can have led to weakening. Oedometer testing gave a hydraulic conductivity of 2.3E-11 m/s.

Disc 10

This disc contained concrete of CBI-type that was investigated with respect to the uniaxial compressive strength, the value obtained being 21.1 MPa.

5.4.2 Comments

Considering the clay distant from the concrete, as represented by Disc 4, it had a hydraulic conductivity that was somewhat higher than that of virgin clay with the same density and a swelling pressure that was slightly lower than that of virgin clay. The samples from Disc 7 also had a conductivity exceeding those of virgin[4] clay but not very much[5]. The relatively small differences in conductivity between virgin clay and the disc clays, and the fact that the swelling pressures were approximately the same indicates that the smectite content and microstructure were not much changed and that cementation effects were insignificant.

The slightly lower hydraulic conductivity of the softest clay (Disc 7) can be explained by precipitated clay/concrete reaction products. The higher swelling pressure may be due to locally higher density in this somewhat heterogeneous part of the plug.

5.5 Results from determination of the chemical properties

The chemical analyses of the clay and concrete samples were comprehensive and are reported separately in APPENDIX A. We will confine ourselves here to present the major findings.

5.5.1 Concrete

Chemical alteration of the cement mineral phases at the clay-concrete contact caused release of Ca and K that had partly replaced Na in the interlayer space of the montmorillonite.

- The cement has clearly been altered in contact with the clay plug and has lost an appreciable part of its mechanical strength.
- In addition to the leaching of Ca and K, neocrystallization of a fibrous Ca-Si phase occurred along with the formation of some amorphous components.
- Comparison of XRD reflections of the altered and unaltered concrete samples shows that a number of reflections in the unaltered sample are smaller or absent in the altered sample. These reflections are attributed to cement phases that either did not crystallize in the altered concrete or have been removed by dissolution.
- Portlandite and possibly belite were recognized and the occurrence of a small amorphous reflection may also indicate new alteration products in the matrix of the altered concrete sample.

5.5.2 Clay

In the central 10 mm part of the clay contacting concrete, precipitation of gypsum and halite occurred forming a salt-rich crust, whereas in the side of the plug, in contact with the granite wall, this crust influenced only the outer 25 μm.

[4] The untreated clay is MX-80, delivered by Clay Technology AB.

[5] The conductivity values were determined using hydraulic gradients ranging between 30 and 50.

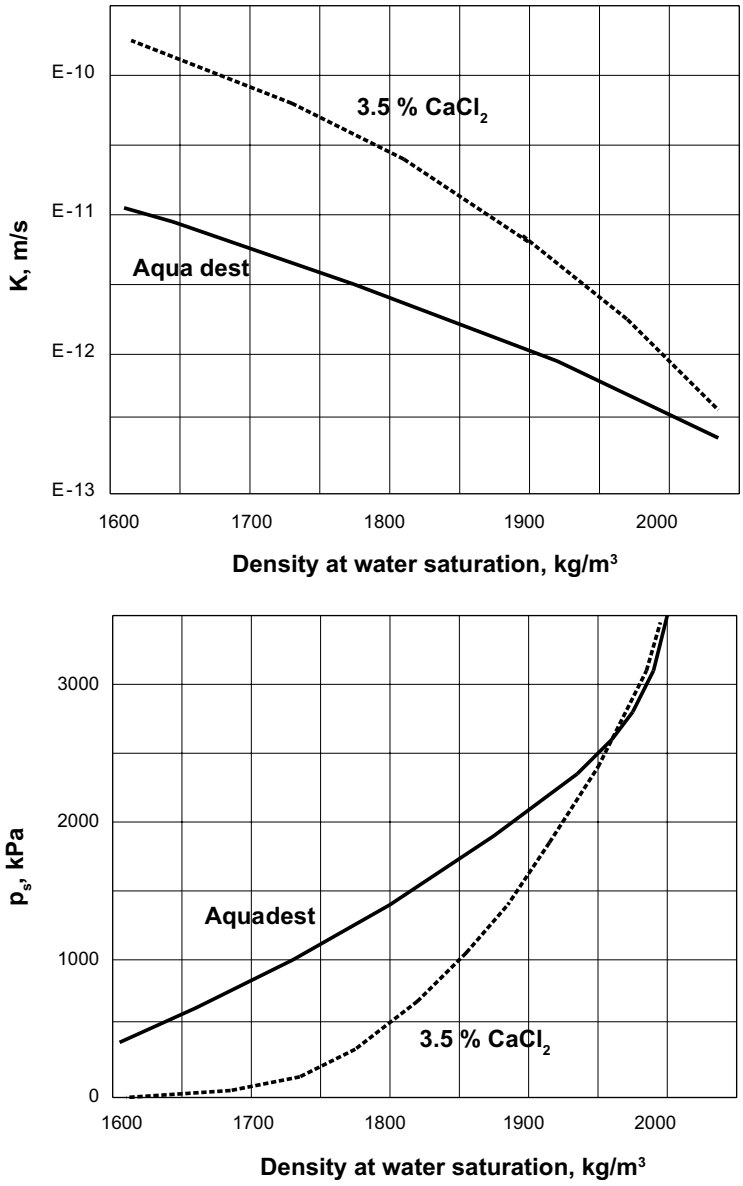

Figure 5-5. *Hydraulic conductivity and swelling pressure of virgin MX-80 clay. The conductivity was determined by using hydraulic gradients of 30–50 (Pusch and Yong 2006).*

- The increase of Ca with decreasing packing density and local occurrence of 2 interlamellar water layers in the clay/concrete contact zone suggest chemical modifications of the properties of the clay.
- The electron microscopy shows that the clay aggregates had a characteristic irregular topography.
- A shift towards higher d-values is observed close to the concrete. It represents the occurrence of more hydrates in the interlayer sites of the montmorillonite due to the exchange of monovalent cations by bivalent ones (e.g. Na^+ exchanged by Ca^{2+}).
- The occurrence of twin XRD peaks of varying intensities within 10 mm of the concrete contact indicates that the montmorillonite interlayers contain heterogeneous mixtures of both bivalent and monovalent cations caused by varying degrees of substitution. This suggests that the cation exchange process is extremely slow and requires tens of years or more to develop fully.
- TEM/EDX analyses reveal the inclusion of a quartz clast at the interface, extending to a depth of about 10 μm, suggestive of ductile flow of the clay.
- The occurrence of salt precipitations reflects desiccation in the region of contact. This indicates limited access to water and low water pressure.

6 Discussion and comments

6.1 Constructability

The field work concerning preparation and placement of concrete and clay plugs could be successfully pursued and the techniques shown to be practical and sufficiently rugged to be recommended for application in other contexts. There were no indications of difficulties in constructing neither concrete nor clay plugs at this shallow depth. The small length of the borehole implies that loss of clay by erosion in the installation phase would be insignificant.

6.2 Physical performance

The major conclusions concerning the performance of the clay plugs were:

- The migration of clay from the interior of the copper tubes to the gap between tube and rock took place according to the predictions; hence leading to a density of the "skin" that was nearly the same as of the "core". This relatively high degree of homogeneity was reached in three years and was probably significant already after half a year.
- The low density of some of the clay plug parts can be explained by axial expansion of the clay to a less dense overlying clay fill. This shows that it is essential to construct plugs so that axial displacements are minimized when applying the borehole sealing technique in deep or long holes.

The major observations respecting the concrete plugs were:

- The compressive strength was significantly lower than implied by CBI data (Pusch and Ramqvist 2007).
- The rock surface in the hole felt oily, which can explain why the adhesive strength was very low. This phenomenon, which may be due to the composition of the concrete, is of utmost practical importance and indicates the need for concrete with inorganic plasticizer.

6.3 Interaction of clay and concrete

6.3.1 General performance

At shallow depth, like in the presently investigated case, the time for maturation of the clay and concrete plugs can be slow depending on the frequency of intersected, water-bearing fractures, while at large depths the higher water pressure speeds up the saturation and makes it relatively independent of the spacing of intersected fractures. Low maturation rates mean that more electrolytes enter the borehole with initially fresh water, which delays homogenization of the clay units and makes the concrete weaker.

The decrease in measured clay packing density towards the concrete contact can be attributed to both physical and chemical changes in the clay. Since there was no confining copper tube at the contact with concrete the clay had to expand into a larger space than the adjacent confined clay but this cannot explain the significant difference in density. Of greater importance is the clear evidence that the bentonite continued to swell and infiltrate the concrete plug after filling of the borehole. Clay was detected both along the contact between the plug and the granite wall as well as interleaved within the bottom of the concrete fill. Such an increase in volume occupied by the MX80 bentonite would be expected to lead to a decrease in the packing density towards the top of the clay plug. It was concluded from the clay analysis that concrete had in fact intruded into the clay. The lesson learned is that the concrete should be more viscous and stiffen quicker than the presently used CBI brand.

6.3.2 Long-term performance

The expected long-term performance of the clay in the larger part of the plugs is at least 100,000 years while the interaction with CBI concrete will lead to significant changes in physical performance. The rate of change of the clay can be roughly estimated assuming that it is controlled by diffusive processes. Thus, applying ordinary diffusion constants – E-10 to E-9 m^2/s – and taking the migration rate of Ca from the concrete to be the driving force it is estimated that clay plugs can undergo significant degradation to a distance from the contact with CBI concrete of 1 m in 500 years and to 2 m in 3000 years. Most of the change is estimated to be an exchange of initially sorbed Na by Ca but dissolution and transformation to nonexpendable clay minerals as shown in the present study will also take place and cause reduction or loss of swelling pressure, while the hydraulic conductivity may not be significantly changed. Concrete with Portland cement would degrade much less, i.e. to a few millimetre distance from the clay in 500 years and to a few centimeters in 3000 years assuming the degradation to be controlled by the dissolution rate of $Ca(OH)_2$. For CBI concrete in boreholes located in rock with Ca-dominated groundwater the rate would probably be lower. The strong retarding effect of larger distance from the clay/concrete contact suggests that further degradation of clay/concrete plugs after a few thousand years is very small.

6.3.3 Overall conclusions and recommendations

The study has demonstrated what chemical and mechanical changes that took place at different distances from the contact between smectite clay and concrete in 3 years. They were relatively small and not substantially damaging the sealing ability of the two components but longer testing time is required to draw safe conclusions on their long-term performances and on the extension of the changes from their contact. A matter of particular importance is the observation that concrete did not adhere to the rock. This requires further investigation.

If the second borehole is plugged in the same way as the presently investigated one further information on chemical, mineralogical and mechanical changes in a longer time perspective will be provided.

References

SKB's (Svensk Kärnbränslehantering AB) publications can be found at www.skb.se/publications.

Pusch R, Ramqvist G, 2004. Äspö Hard Rock Laboratory. Borehole sealing, preparative steps, design and function of plugs – basic concept. SKB IPR-04-57, Svensk Kärnbränslehantering AB.

Pusch R, Ramqvist G, 2007. Borehole projects – Final report of Phase 3. SKB R-07-58, Svensk Kärnbränslehantering AB.

Pusch R, Yong R N, 2006. Microstructure of smectite clays and engineering performance. New York: Taylor & Francis.

Pusch R, Zwahr H, Gerber R, Schomburg J, 2003. Interaction of cement and smectitic clay – theory and practice. Applied Clay Science 23, 203–210.

Appendix A

Sealing of Investigation Boreholes:
Mineralogical and geochemical borehole plug analyses

SKB Report (30.04.2010)

Economic account number TU02

A1 Scope of the study

This report presents the results from mineralogical and geochemical analyses of selected samples taken from the clay and CBI concrete plug extracted from a 5 year old granite borehole at 220 m depth that was recovered in December 2009. The positions of the sampled discs are shown in Figure A-1, along with the measured clay packing density variations.

Two primary features of interest that require explanation are:

i) The decrease in the measured clay packing density (for the moist samples) towards the concrete contact, which decreases from 2,000 kg/m^3 in disc 4 to 1,800 kg/m^3 at the top of disc 7.

ii) The cause of the extensive alteration of the cement at the contact with the clay (disc 7) that has led to lose of its material strength.

To address these two features, we have performed a detailed X-ray diffraction (XRD), X-ray fluorescence (XRF) and electron microscopy study (both scanning and transmission electron microscopy: SEM, TEM) on the sample material. The analytical results provide constraints on the mineralogical and geochemical variations in both the concrete and clay materials that can be used to assess both the cause of the clay packing density changes and cement alteration at the clay-concrete interface. In addition to these studies, we have also conducted some state-of-the-art dual beam (combined ion and electron) microscopy for characterizing the distribution of elements and mineral particle textures in a cut section within the outer 40 micron wall of the clay plug: the site of intense chemical activity.

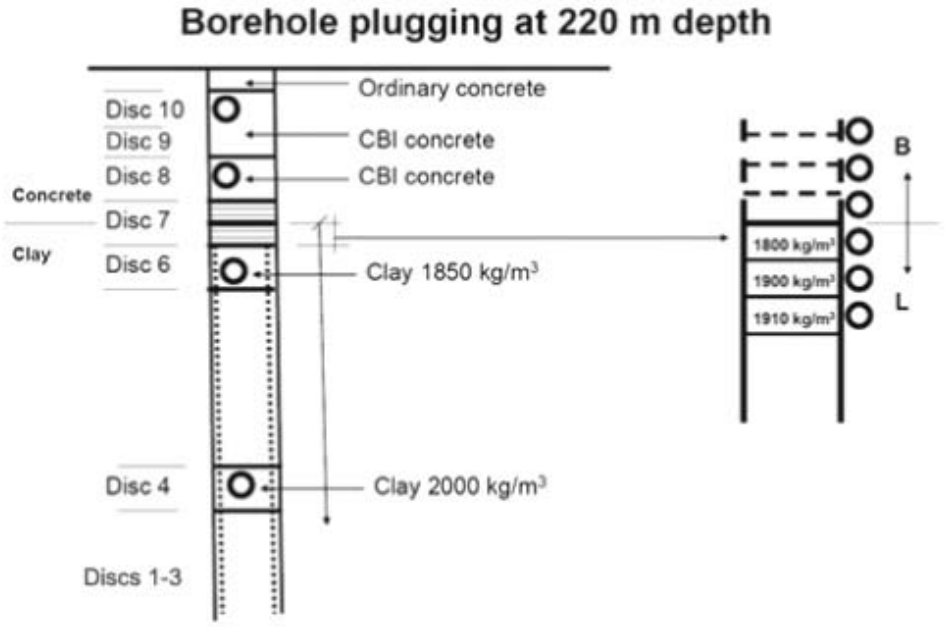

Figure A-1. *Position of the discs sampled from the borehole plugging at 220 m depth. The wet packing densities of the clay are shown expressed in kg/m^3 (available from Roland Pusch).*

A2 Sampling and analyses

Samples were extracted from the disc cores using both hammer and tweezers. Any visual signs of contamination were removed with a fine brush under the binocular microscope. Small clay and concrete fragments (upto 3–5 g) were crushed using a ball mill for typically 15 to 30 minutes to produce a fine-powder for XRD and XRF study. Small quantities of this powder were also used for TEM investigations. For scanning electron microscopy and dual beam study, three samples were prepared from the interface area of the clay, concrete and granite from disc 8 (Figure A-2). The clay sample of MX80 bentonite (A) shows a flat surface that represents the direct contact with the granite and was sampled in close proximity with the strongly altered concrete plug. A thick section through this portion of the plug (B) was also prepared in our rock laboratory and the flat upper surface polished. One edge of the slab was also polished, so that the sharp corner, representing the corner closest to the interface with the clay, could be studied. A granite sample from the borehole wall was also prepared in this way, but this sample was not here studied in detail.

In addition to these samples, altered and unaltered chips of the concrete were also investigated by SEM. These 3–5 mm pieces were selected on the basis of showing clean but rough uneven surfaces ideal from secondary electron imaging. A summary of the key samples and the analytical methods that were applied to them are shown in Table A-1. As the data base is an extensive one, only the key results are included in this report or in the Appendix. The results from the analyses of individual samples are available from the laboratory on request.

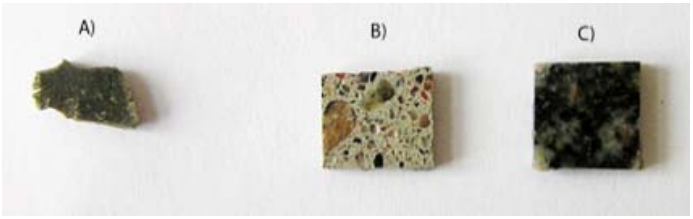

Figure A-2. *Solid rocks samples prepared from the interface area between the clay and concrete and the granite wall of the borehole.*

Table A-1. Summary of samples studied and the analytical techniques used. XRD = X-ray diffraction, XRF = X-ray fluorescence, SEM = scanning electron microscopy, TEM = transmission electron microscopy.

Sample	Disc	XRD Powder	XRD Texture	XRF	SEM	TEM	Comments
Concrete (C)							
C10	10	X	X	X		X	Unaltered concrete
C9	9	X		X	X	X	Unaltered concrete
C8a	8	X		X	X	X	Altered concrete
C8b	8	X	X	X	X		Altered concrete
Smectite (S)							
S7cC	7	X	X	X			Contact with concrete
S7cC-2	7	X	X	X			Contact with concrete
S7cG	7	X	X	X			Clay contact with granite
S7a	7	X	X	X		X	contact concrete, packing density 1,800 g/cm^3
S7b	7	X	X	X		X	contact area, packing density 1,900 g/cm^3
S7c	7	X	X	X		X	contact area, packing density 1,910 g/cm^3
S6	6	X	X	X			Fresh clay
S4	4	X	X	X			Fresh clay, packing density 2,000 g/cm^3
S3	3	X	X	X			Fresh clay
S2	2	X	X	X			Fresh clay
S1	1	X	X	X			Fresh clay
Granite (G)							
G	8	X		X			Fresh granite sample from margin of borehole

A3 Analytical techniques

X-ray diffraction

Random powder XRD analyses were made by packing the crushed powder into plastic XRD holders and by sideward tapping to enhance random particle orientations. Standard measurements between 2 and 50°2θ angles at 0.02° step sizes and 2 seconds count time per step were made using a Siemens/ Bruker D5000 diffractometer housed with an automatic sample changer. The EVA software combined with the PDF2 database from the International Centre for Powder diffraction data was employed for phase identification and presentation of the results. Textured (oriented) preparations of the clay samples were made by first drying the samples overnight at 60°C and then 30 mg of powder weighed and mixed with 1 ml of distilled water. After ultrasonic treatment and mechanical mixing, the clay-in-suspension was pipetted onto a 3×3 cm glass slide and left to dry overnight. This produced a thin clay film where the smectite particles have a high degree of preferred orientation suitable for the study of their basal XRD reflections (Moore and Reynolds 1987). XRD measurements of the textured slides were typically made between 2 and 30°2θ angles using 0.02 step sizes and 2 s count time. The measurements were also made under conditions of similar laboratory humidity (ca 30%).

X-ray fluorescence

A weight of 0.8 g powder was heated to 1,030°C for 10 minutes in the oven to remove volatiles (mainly H_2O and CO_2) and then mixed with 4 g lithium metaborate in platinum cups and reheated to 1,200°C for a further 10 minutes until the solids were digested. The loss-on-ignition was determined by gravimetric analyses of the samples with measurement made at 105° and 1,000°C. The fused tablets were then analyses using a Phillips XRF instrument Type PW 2404. A range of USGS standards (AGV-2, RGM-1, FK and BCR-2) were run at the beginning and after the sample run to determine any variations in the measurements (Brown et al. 1973).

Electron microscopy

SEM study was undertaken using a JEOL JXA-840A instrument. Palladium coated rock fragments were studied using secondary electron imaging supported by energy dispersion X-ray (EDX) spectroscopy. For combined electron and ion beam study, both a Quanta™ 3D 200i from FEI and an Auriga microscope from Zeiss were used. These instruments allow for combined imaging and cutting capabilities and are capable of producing serial imaging and analyses suitable for 3D reconstructions. TEM microscopy was undertaken using a JEOL JIM 1210 equipped with a new Orion CDD camera for real time imaging. Samples were first dispersed in distilled water and then a very dilute suspension of clay-in-solution was dropped onto a carbon film stretched over a TEM copper grid. Following carbon coating, the particles of the samples can be studied in the areas of the holds of sample grid. The microscope allows for combined imaging, EDX analyses and selected areas electron diffraction (SAED) investigations, which was here conducted a magnifications of around ×30,000.

A4 The smectite clay (MX80 bentonite)

XRD results

Table A-2. Summary of important aspects of the XRD results: Mnt = Montmorillonite (smectite), FWHM = Full-width-at-half-maximum.

Sample	Mnt d-value (001) Å random powder	FWHM Δ°2θ	Mnt d-value (001) Å oriented	FWHM Δ°2θ	Comment
S7cC	12.80	0.66	14.97	1.15	2 water layer Ca Mnt. Some gypsum in whole rock
S7cC-2	–	–	12.74	1.47	1 and 2 water layers in interlayer
S7cG	12.92	0.78	–	–	1 and 2 water layers in interlayer
S7a-tx-ad	–		12.48	1.00	Dominantly 1 water layer
S7b-tx-ad	–	–	12.50	1.27	Dominantly 1 water layer
S7c-tx-ad	–	–	12.48	0.91	Dominantly 1 water layer
S6-txt	10.18	–	12.50	1.14	Dominantly 1 water layer
S4-txt	10.22	0.75	12.45	0.99	Dominantly 1 water layer
S3-txt	11.10	–	12.56	0.98	Dominantly 1 water layer
S2-txt	10.30	–	12.55	0.95	Dominantly 1 water layer
S1-txt	11.73	–	12.57	1.02	Dominantly 1 water layer

The XRD patterns of the first basal reflection (001) of montmorillonite for random powder and oriented texture preparations are presented in Figures A-3 and A-4, and the measured d-values and FWHM (Full-width-at-half-maximum) parameters summarized in Table A-3. A shift towards higher d-values is observed in the upper part of disc 7, close to the concrete, both in the random powder and oriented clay preparations. This shift represents the occurrence of more water-layers in the interlayer sites of the montmorillonite due to the exchange of monovalent cations by bivalent ones (e.g. Na^{+} exchanged by Ca^{2+}). In the random powder preparation, this feature is seen by the 12.80 and 12.92 Å d-values of the smectite clay samples directly (< 10 mm) at the contact with the concrete (Figure A-3). These values are notably higher than the 10.18–11.73 Å range of values for the samples located deeper in the clay plug. The occurrence of more water-layers in the contact clay is also revealed in the textured clay preparations, where the oriented montmorillonite particles allow determination of the thicknesses of the water-layers in the crystallographic c*-direction to be resolved (Warr and Berger 2007). Here the ca 15 Å reflection indicates a 2 water layer structure dominates whereas the 12.45 to 12.57 Å range represent 1 water layer structures. The occurrence of both these peaks of varying intensities within 10 mm of the concrete contact indicates that the montmorillonite interlayers contain heterogeneous mixtures of both bivalent and monovalent cation caused by varying degrees of substitution. Such mixtures are responsible for the broader 001 reflections with higher FWHM values >1.00 Δ°2θ (Table A-2).

XRF results

The XRF results expressed as weight % oxides are presented in Table A-3 and plotted in Figure A-5. The samples shown strong fluctuations in the amount of volatiles (LOI) lost during heating to 1,000°C, which is typical for Wyoming based bentonite samples (Mermut and Cano 2001). There appears to be no obvious relationship between the LOI values and the position of the samples in clay plug. As the main volatile content in these samples is however water, the measured variations are most likely related to the complex dehydration behavior of the bentonite powders during heat treatment (Guggenheim and van Groos 2001). The clay samples of disc 7 collected close to the contact with the concrete plug show localized enrichments in Mg, Ca, Na and K and some depletion in Al and Fe compared with the fresh bentonite clay of discs 1–6. One exception to this pattern is the highest percentage of CaO record in sample S1 from disc 1. This enhanced value may relate to sample contamination or heterogeneities due to some gypsum precipitation.

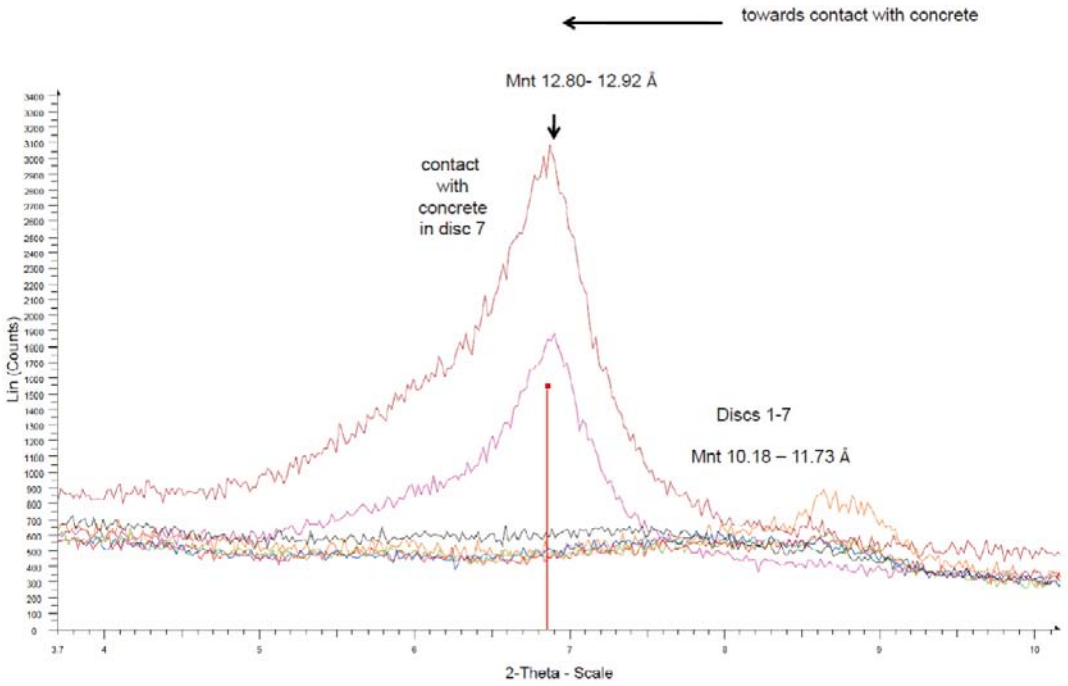

Figure A-3. *XRD patterns of the 001 montmorillonite reflection from random powder preparations. Higher intensity reflections with larger d-values are recorded at the contact with the concrete.*

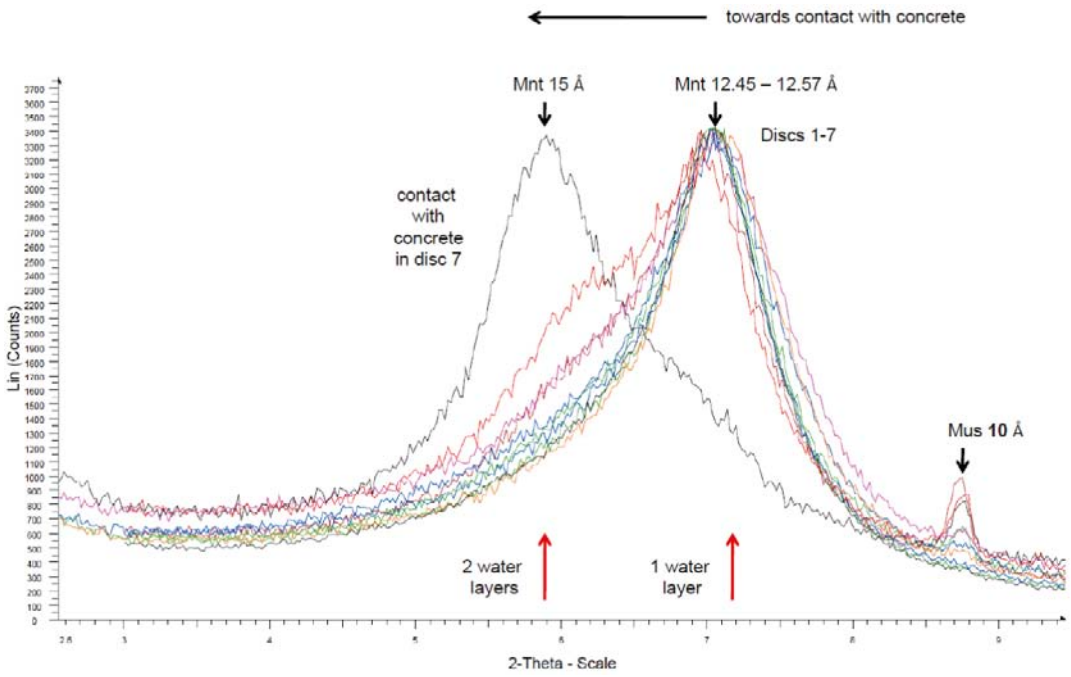

Figure A-4. *XRD patterns of the 001 montmorillonite reflection from textured clay preparations. The clay in contact with the concrete indicates 2 water layers dominates the interlayer compared to the 1 water layer structures detected deeper in the clay plug.*

In this study, the concentration of trace elements was also measured (see Appendix for results). As the implications of these results do not lie within the main context of this report, the trace element geochemistry is not considered here.

Differences in the weight % of CaO do occur in the upper part of disc 7 (S7a–S7c) towards the contact with the concrete plug. In Figure A-6 the increase in Ca correlates roughly with the measured decrease in packing density. This could represent some incorporation of Ca into the interlayer of the montmorillonite and a related loss of swelling pressure or alternatively it may reflect the circulation of more concentrated electrolytic solutions and subsequent precipitation of salts (e.g. gypsum and halite) that can also suppress the amount of osmotic swelling in the MX80 bentonite. Both these mechanisms cam result in lower packing densities of the clay, but as these particular samples do not show the development of the typical 2 water layer structures in the XRD patterns expected for Ca-montmorillonite (Table A-2) and do show enhanced Na concentrations, the latter mechanism is considered the more likely explanation.

Table A-3. XRF results of the MX80 bentonite samples including LOI values.

Sample	SiO2 (%)	TiO2 (%)	Al2O3 (%)	Fe2O3 (%)	MnO (%)	MgO (%)	CaO (%)	Na2O (%)	K2O (%)	P2O5 (%)	LOI (%)	Sum (%)
S7cC	63.54	0.19	16.43	3.08	0.02	2.46	1.55	2.31	1.25	0.07	7.93	98.81
S7cC-2	54.22	0.15	17.05	3.16	0.01	2.34	1.44	1.94	0.57	0.06	15.23	96.15
S7cG	56.41	0.16	16.64	3.21	0.01	2.19	1.46	2.00	0.80	0.06	7.39	90.32
S7a	60.95	0.16	19.52	3.72	0.01	2.29	1.52	3.16	0.64	0.06	6.78	98.82
S7b	60.70	0.16	19.54	3.71	0.01	2.23	1.50	2.01	0.56	0.06	6.83	97.30
S7c	60.08	0.16	19.39	3.63	0.01	2.20	1.49	2.09	0.57	0.06	7.59	97.26
S6	54.58	0.15	17.60	3.23	0.01	1.99	1.40	1.93	0.57	0.06	9.86	91.38
S4	59.89	0.16	19.34	3.65	0.01	2.30	1.30	2.17	0.57	0.06	7.15	96.59
S3	59.84	0.16	19.13	3.56	0.01	2.25	1.38	2.17	0.62	0.07	9.45	98.64
S2	59.43	0.17	19.09	3.55	0.01	2.27	1.39	2.19	0.60	0.06	9.36	98.12
S1	58.30	0.16	18.71	3.52	0.01	2.26	1.63	1.77	0.58	0.06	10.86	97.87

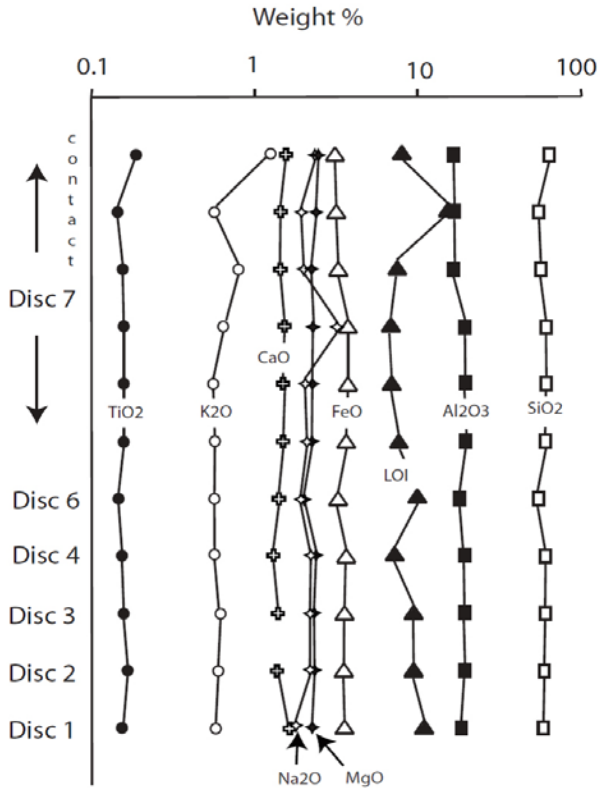

Figure A-5. *Variation in weight % oxides in the different discs sampled with plug depth.*

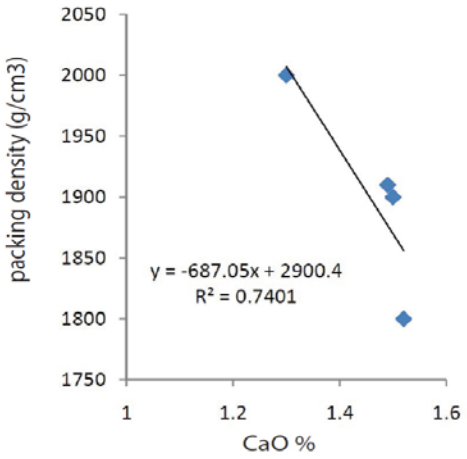

Figure A-6. *Variation in weight % CaO with packing density.*

Electron microscopy and ion beam sectioning

A series of serial cuts 40 µm long were made with an ion-beam into the upper surface of the soft MX80 bentonite sample (S7cG) that represents the contact between clay and granite close to the position of the cement plug (Figure A-7). This section reveals the inclusion of a quartz clast (darker grey) at the interface, extending to a depth of ca 10 µm, suggestive of ductile flow of the clay. The occurrence of salt precipitations in the outer layer (light grey) also reflects desiccation in the region of contact.

A 3D reconstruction of the serial cutting reveals the largely random orientation of montmorillonite particle stacks that are separated by intervening microporosity (Figure A-8). The local alignment of clay platelets at the border of the included clast (top left of section) probably reflects the flow alignment of the particles as the bentonite swelled and pushed against the granite borehole wall. In the 3D view, the pores are also observed to be non-connected and lens-shaped, with an average length of

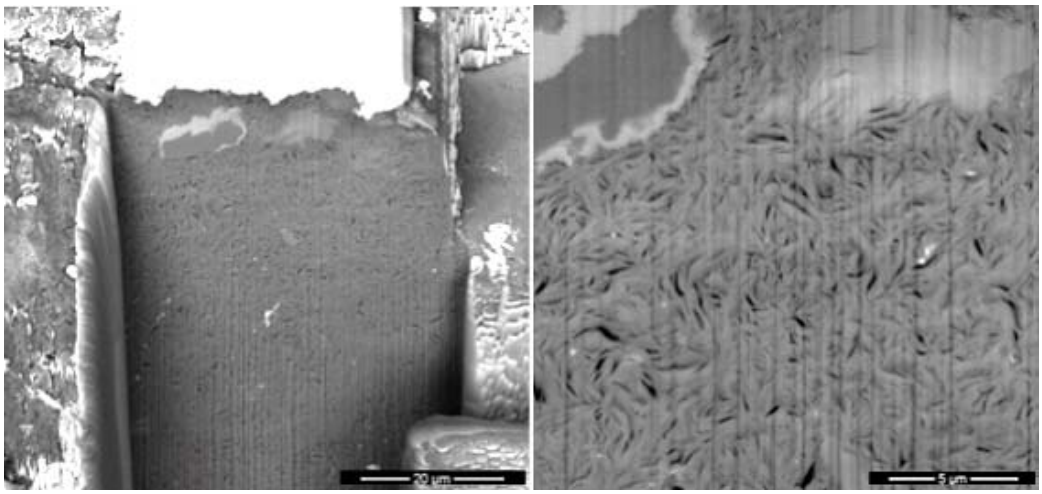

Figure A-7. Serial cross-sectioning of the bentonite sample with backscattered electron beam imaging of the cuts.

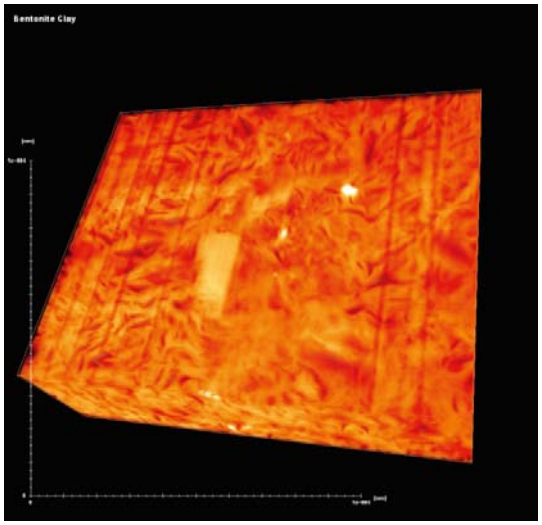

Figure A-8. Three dimensional reconstruction of the bentonite clay fabric revealing the largely random orientation of montmorillonite particles and the intervening micro-porosity in the dehydrated state.

ca 1 µm. Such information could be used to estimate pore connectivity and combined with chemical data allow reconstruction of reactive transport paths in this material. As determining the rates and mechanisms of both elemental mobility and retention in bentonite clay is of great importance to the waste disposal industry, this type of analytical study can bring significant new insights into this field of research.

The EDX mapping of one of the cross-section cuts successfully reveals the distribution of elements away from the contact surface (Figure A-9). The upper region appears to show higher concentrations of both Ca and Na, probably representing chloride salt precipitations. The continuous decrease in Ca downward in Figure A-9, into the clay material, is caused by the diffusion of this element released by alteration of adjacent cement. It most likely replaces other cations (such as Na) within the interlayer sites of the montmorillonite clay particles. In this cut, the distance of Ca diffusion appears to influence most the outer ca 25 µm of the bentonite filled core that was in contact with the side of the granitic borehole.

A second cut into another bentonite fragment sampled from the wall of the clay plug was made by milling 15 slices, each with a thickness of 100 nm and a pixel size of 27.91 nm (Figure A-10). This cut was place a little closer to the clay contact with the granite and more successfully images the interface region.

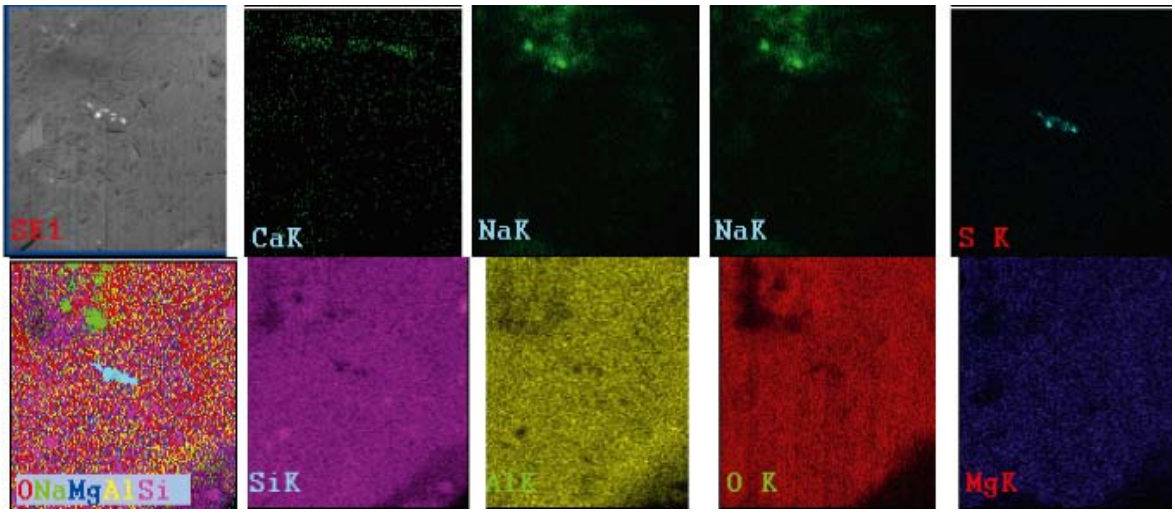

Figure A-9. *EDX mapping of one of the serial cuts into the bentonite clay. The upper border of the analyzed area lays 5 µm from the clay-granite interface.*

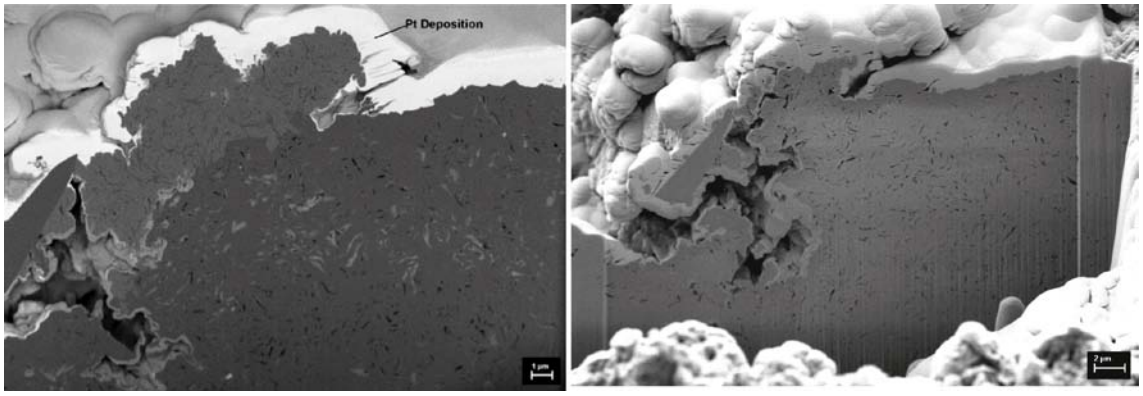

Figure A-10. *Left. Energy sensitive backscatter image of the upper part of the bentonite clay at the contact with the granitic wall of the borehole. Right. Secondary electron image of the cut section.*

The serial cutting shows a nice upper crust of clay just 5 µm thick (lighter shade of grey in the top left hand corner of Figure A-10) and small, lenses shaped precipitations trapped within pore spaces. As a broader range of elements were mapped by EDX (Figure A-11), there precipitations can be identified as gypsum and halite, respectively.

The secondary electron image of the surface (Figure A-12), which shows the early stages of ion beam thinning, reveals a series of platy encrustations and clasts that lie on the surface. The clay aggregates also has a characteristic irregular topography probably resulting from flocculation in the presence of strong salt solutions.

A5 The concrete plug

XRD results

The XRD patterns of the random powder preparation of the concrete samples are dominated by the large amount of crushed granite contained within this material that hindered recognition of the cement phases using this technique. To overcome this problem, the concrete samples were placed in a glass beaker with distilled water and ultrasonically treated to separate and disperse the fine cement phases. After ca 15 minutes of treatment, the coarser suspension was allowed to settle and the finer suspended material was separated, concentrated, and pipetted onto glass slides for XRD study.

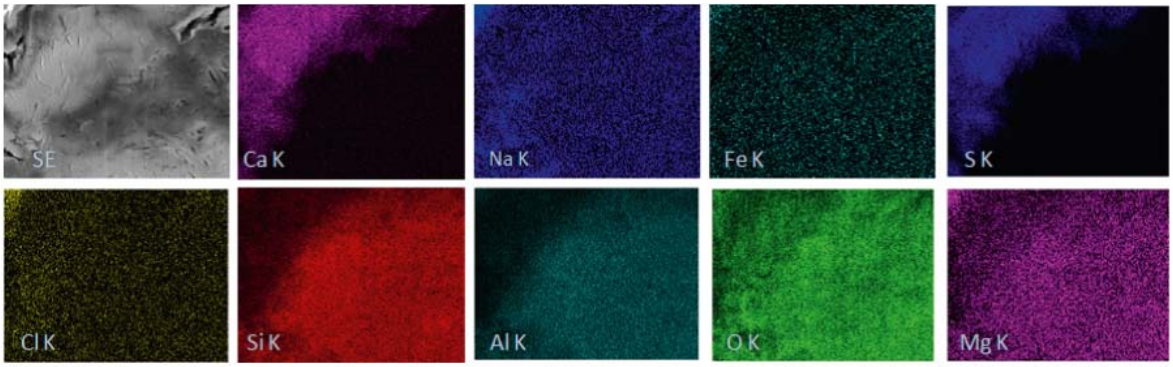

Figure A-11. *EDX mapping of one of the serial cuts into the bentonite clay. The upper left corner marks the clay-granite interface.*

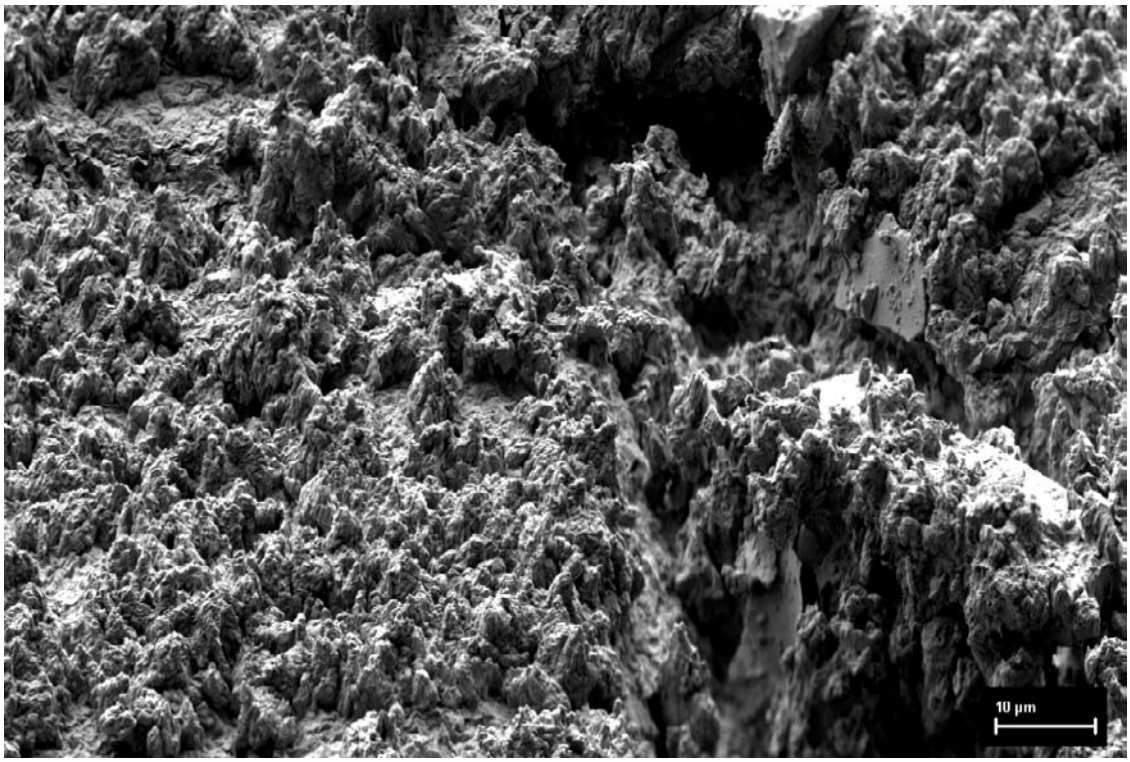

Figure A-12. *Secondary electron image of the surface of the bentonite clay showing encrusting salts and flocculation of the clays due to the presence of strong salt solutions.*

A comparison of the altered (C8) and unaltered (C9) concrete samples is shown in Figure A-13, which reveals a number of XRD reflections in the unaltered sample that are smaller or absent in the altered sample. These reflections are attributed to cement phases that either did not crystallize in the altered concrete or have been removed by dissolution. Although all of the phases could not be identified due to the complexity of the XRD patterns, portlandite and possibly belite were recognized based on reflections at 4.9 Å and 2.8 Å. The occurrence of a small amorphous reflection between 5.5 and 7°2θ may also reflect new alteration products in the matrix of the altered concrete sample that are not detectable in the unaltered material (Figure A-13).

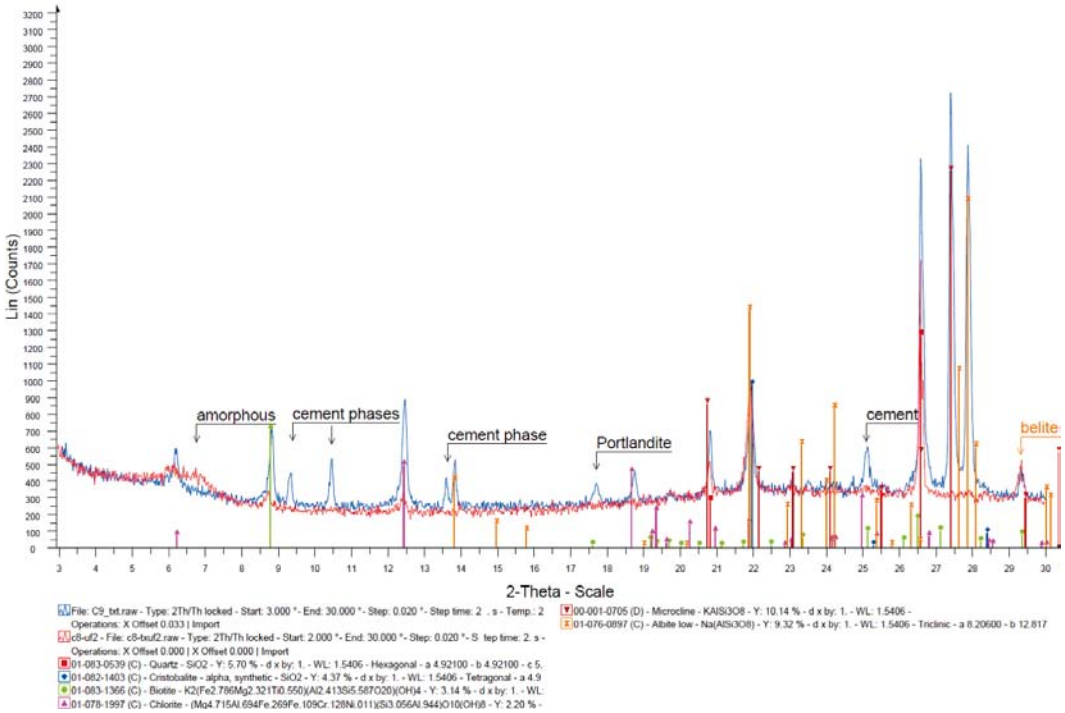

Figure A-13. *XRD patterns of the altered (C8) and unaltered (C9) concrete samples following ultrasonic treatment and sedimentation of the fine-grained fraction performed to concentrate cement phases.*

XRF results

The XRF results of two altered (C8a and C8b) and two unaltered (C9 and C10) concrete samples are presented in Table A-4. The altered samples are notably depleted in Si, Ca and K but all other elements have similar amounts in both sets of samples. The main fluctuations in the elemental data are probably due to the heterogeneous nature of the large volumes of granite in the concrete, which is expected to mask any elemental differences due to cement chemistry.

SEM results

Selected rock fragments with freshly broken surfaces of unaltered and altered cement were investigated by SEM. The cement appears white to light grey in secondary electron images due to the poorly conductive porous calcium oxides phases (Figure A-14). The unaltered C9 concrete sample shows a clear matrix of cement phases that coat grain surfaces (Figure A-14a). The cement has a porous granular appearance and is composed typically of Ca-Si phases, probably calcium silicate hydrate (C-S-H), with traces of Fe, K, and Al that may reflect contamination of the analyses from granite derived minerals in the concrete (Figure A-14d). Similar types of porous cement phases are observed in the altered cement sample C8 (Figure A-14b), but these patches show signs of strong dissolution and neocrystallization of a fibrous CaSi phases, also with some Fe, K and Al present in the analyses. The composition of this phase is notably richer in Ca than the granular cement and may result from more prolonged hydration of Portland cement phases (Kjellsen et al. 2004). Whether or not the formation of this fibrous cement phases is related to the breakdown of the cement during alteration is unclear, but there is clear evidence for strong dissolution of the granular cement phases responsible for the generally lower Ca concentration detected in the bulk sample (Table A-4).

Table A-4. XRF results of the concrete samples including LOI values.

Sample	SiO2 (%)	TiO2 (%)	Al2O3 (%)	Fe2O3 (%)	MnO (%)	MgO (%)	CaO (%)	Na2O (%)	K2O (%)	P2O5 (%)	LOI (%)	Sum (%)
C10	74.29	0.31	9.62	2.69	0.04	1.02	3.74	1.70	2.84	0.12	4.06	100.42
C9	73.80	0.26	10.79	2.45	0.03	0.92	2.94	2.36	2.98	0.09	2.84	99.46
C8a	72.92	0.27	10.37	2.52	0.04	0.92	2.58	2.22	2.70	0.09	2.57	97.18
C8b	70.42	0.26	10.33	2.38	0.04	0.98	3.12	2.10	2.70	0.09	4.64	97.06

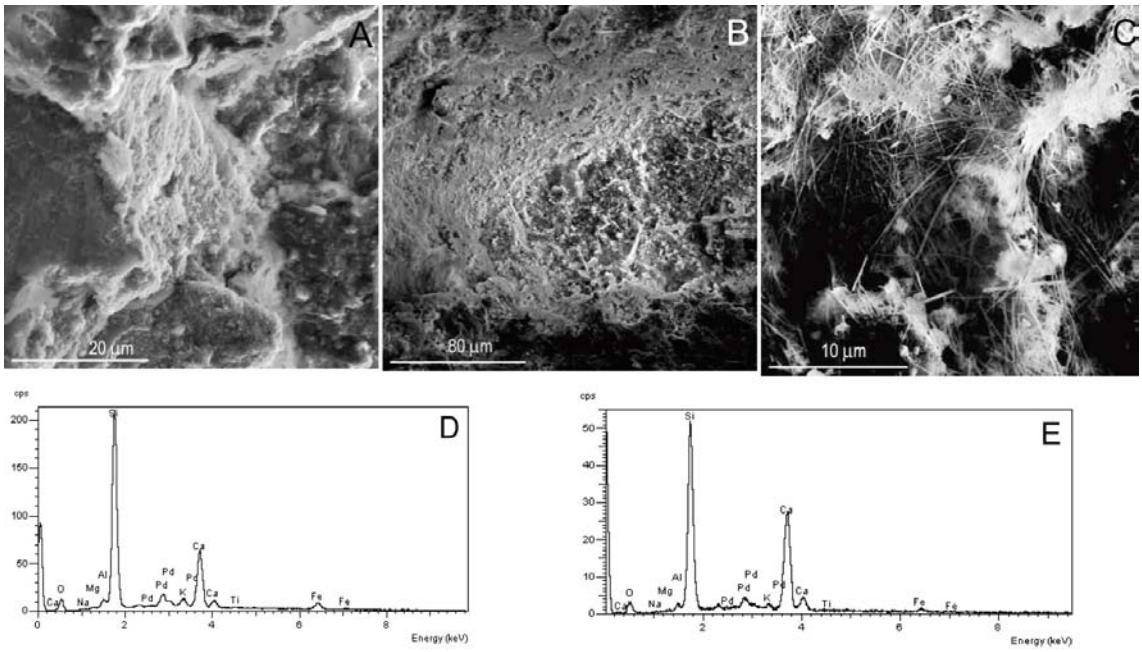

Figure A-14. *SEM (secondary electron) images of A) unaltered cement (C9) and B) altered cement (C8). The white areas represent porous Ca-oxide cement phases. C) A higher magnification image of the altered cement showing a neocrystallized fibrous cement phase, which was not detected in the unaltered sample. D) EDX spectrum of the unaltered cement (C9) shown in image A). E) EDX spectrum of the altered cement (C9) shown in image C).*

TEM results

A comparison between the unaltered (C10) and altered (C8) concrete sample was made by TEM study (Figure A-15). A higher proportion of finer particles were observed in the altered cement, together with contamination by montmorillonite. The small aggregated particles (e.g. G) with hollow inner structures were not observed in the unaltered sample, suggestive of possible formation of new alteration products. A large portion of the material is either small fragments of the crushed granite, fine α-quartz or spherical balls of cristabolite. Cement phases were not commonly encountered and proved difficult to identify due to the large degree of contamination incurred during EDX analyses. In order to determine any composition differences between the two samples, over 100 particles per sample were analyzed by EDX but only a few of these analyses are considered to represent Ca-rich-cement phases, such as some possible Portlandite $Ca(OH)_2$ in Figure A-15 (left image, grain H).

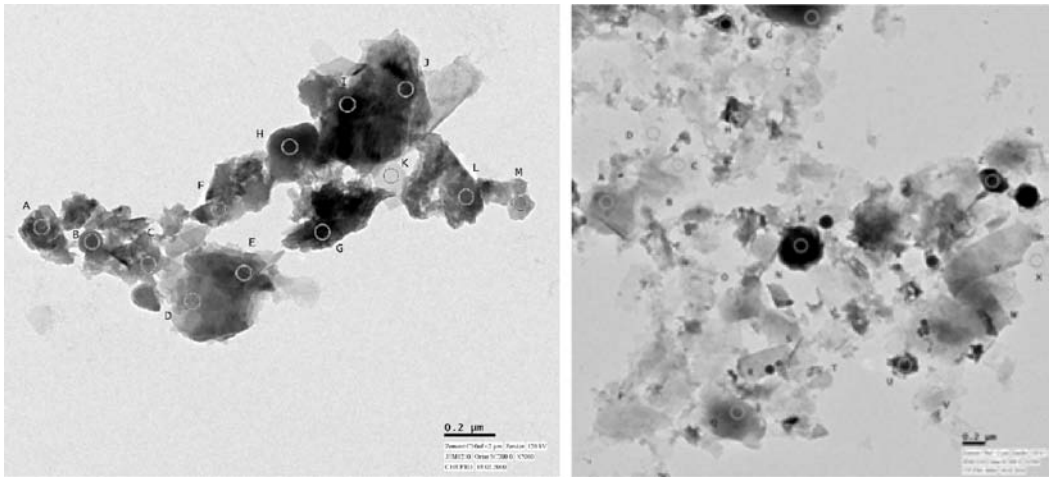

Figure A-15. *TEM image of the fine fraction (<2 micron) ultrasonically extracted from the unaltered cement (left: C10) and altered cement (right: C8). Grain H in the left image is a Ca-rich cement phase (possibly portlandite).*

A6 Conclusions

1. The decrease in the measured clay packing density (for the moist samples) towards the concrete contact can be attributed to both physical and chemical changes in the bentonite. There is clear evidence that the bentonite continued to swell and infiltrate the concrete plug after filling of the borehole. Clay is detected both along the contact between the plug and the granite wall as well as interleaved within the bottom of the concrete fill. Such an increase in volume occupied by the MX80 bentonite would be expected to lead to a decrease in the packing density towards the top of the clay plug.
2. Chemical alteration of the cement mineral phases at the clay-concrete contact released some quantities of Ca and K that have partly replaced Na in the interlayer of the montmorillonite in the upper part of the clay plug in disc 7. In the upper <10 mm of the clay, precipitation of gypsum and halite occurs forming a salt-rich crust, whereas in the side of the plug, in contact with the granite wall, this crust influences only the outer 25 μm. The increase of Ca with decreasing packing density and the local occurrence of 2 water layers in the interlayers of the montmorillonite in the contact zone suggest chemical modifications of the properties of the sealant bentonite have occurred.
3. The cement has clearly been altered in contact with the clay plug and has lost its material strength. In addition to the leaching of Ca and K, the neocrystallization of a fibrous Ca-Si phase occurs along with the formation of some amorphous components. Dissolution in strong saline waters is the probable mechanism of cement weakening in the plug, although the stresses generated by the continued swelling of the bentonite may have also inhibited adequate cementation reactions.

A7 References

Brown G C, Hughes D J, Esson J, 1973. New X.R.F. data retrieval techniques and their application to U.S.G.S. standard rocks. Chemical Geology 11, 223–229.

Guggenheim S, van Groos A F K, 2001. Baseline studies of the Clay Minerals Society source clays: thermal analyses. Clays and Clay Minerals 49, 433–443.

Kjellsen K O, Justnes H, 2004. Revisiting the microstructure of hydrated tricalcium silicate – a comparison to Portland cement. Cement & Concrete Composites 26, 947–956.

Mermut A R, Cano A F, 2001. Baseline studies of the Clay Minerals Society source clays: chemical analyses of major elements. Clays and Clay Minerals 49, 381–386.

Moore D M, Reynolds R C, 1997. X-Ray diffraction and the identification and analysis of clay minerals. 2nd ed. Oxford: Oxford University Press.

Warr L, Berger J, 2007. Hydration of bentonite in natural waters: application of "confined volume" wet-cell X-ray diffractometry. Physics and Chemistry of the Earth, Parts A/B/C 32, 247–258.

Appendix B

XRF data: trace elements

Sample	Ba*	Ce*	Co*	Cr*	Cs*	Cu*	Ga*	Hf*	La*	Mn*	Mo*	Nb*	Nd*	Ni*	Pb*	Rb*
C10	518	72	22	72			10	< 5	33		< 3	9	21	22	21	104
C9	484	68	6	60			11	8	30		< 3	9	24	16	20	122
C8a	439.3	48.6	12.3	49.5	–2.8	2.7	11.4	7.3	39.2	289.1	–0.4	8.4	24.6	14.7	22.9	111.8
C8b	452.4	53	4.8	66.6	5.6	16	10.9	3.3	30.2	271.9	0.2	7.7	18.4	11.5	22.4	110.1
S7cC	369	103	< 5	228			22	8	46		< 3	26	40	< 5	41	46
S7cC-2	311	89	< 5	155			23	9	45		< 3	23	38	< 5	49	15
S7cG	311	91	8	224			23	< 5	31		4	22	40	38	43	26
S7a	394.9	100	2.2	308.6	1.7	2.6	28.1	10.1	62.3	92.6	0.1	26.5	41.8	14.4	52.6	16.1
S7b	354.5	115.7	1.2	228.1	2.6	1.8	29.3	8	49.8	87.9	0.6	27.5	42.9	25.7	52	16
S7c	337.9	110.4	0.8	191.1	17.3	–1.4	26.4	10.3	51.9	79.5	–0.3	27	42.4	9.6	52.8	15.4
S6	356	110	12	51			24	12	40		< 3	23	35	< 5	48	15
S4	317.5	108.5	2.1	303.6	18.2	0.5	28.2	11.4	51.1	81.4	0.3	25.7	40.4	11.3	47.3	16.5
S3	412	105	7	41			26	9	44		< 3	26	49	< 5	55	16
S2	426	109	49	160			32	8	72		3	26	48	< 5	53	15
S1	424	117	< 5	61			25	6	44		< 3	25	42	< 5	54	17

Sample	Sc*	Sn*	Sr*	Ta*	Th*	U*	V*	W*	Y*	Zn*	Zr*
C10	–2		225	0	13	4	53	< 5	28	53	165
C9	8		205	–3	12	5	43	7	20	45	119
C8a	8.5	–27.3	187.8	–1.9	19.7	3.4	32	0.9	26	52.1	137.4
C8b	6.3	–10.1	191.1	–1	18.7	4.3	41.4	–0.9	33.4	51.3	103.5
S7cC	3		220	7	34	11	13	< 5	40	81	177
S7cC-2	1		202	3	39	12	12	< 5	41	102	190
S7cG	0		207	2	36	10	16	< 5	41	100	176
S7a	3.4	9.9	277.2	4.9	46	15.3	8.9	1.8	49.7	111.7	194.2
S7b	5.6	14.2	283.1	–1	46.6	14.8	6.2	–0.4	49.7	116.9	188.9
S7c	3.6	–3	278.9	1.8	46.1	15	7.3	2.8	46.9	111.2	199.4
S6	–2		272	2	38	13	< 12	< 5	35	94	195
S4	9.9	3.2	272.7	2.4	44.8	14	8	0.7	46.1	121.5	184.6
S3	4		310	1	42	14	< 12	< 5	42	102	228
S2	6		293	4	46	11	< 12	7	41	108	216
S1	1		335	0	48	15	< 12	< 5	53	101	222

Appendix C

Daily log

09	Version 3.0.0
	DAILY LOG
	Page__1__of_____

SITE Äspö	PROJECT Slitsborrning	CREW MEMBERS Jan Hultgren Nils Göran Myren NCC Construction
RESPONSIBLE IN FIELD(full name) Patrik Hagman	RESPONSIBLE ORGANIZATION SKB	
ADDITIONAL DATA(not compulsory)	ACTIVITY PLAN NO: **TU 02**	

Date (yymmdd)	Time		Activity	time	name	Section number (In bore-hole)	Position along object	
	Start (hh:mm)	Stop (hh:mm)					From (m)	To (m)
100113	07,00	16,00	Förberedelser inför sågning. Uppriggning provkropp och vajersåg pressening med värme under mot frysning.	7,0	JH			
100114	07,00	16,00	Sågning för provtagning.Start 10,30 förstasnittet klart11,45.Därefter mätningar insjusteringar. Vi körde 5 snitt denna dag och plastade in 4 prover. Plastade även in mellanbitar. Snitt 1 var 10 cm från botten prov 1 botten kopparrör. Snitt 2 var 120 cm från botten. Snitt 3 var 126 cm från botten prov2. Snitt 4 var 131 cm från botten prov 3. Snitt 5 var 139 cm från.	8,0	JH			
100115	07,00	15,00	Förberedelser ny vajer.Start 08,00 snitt 6 var 230 cm från botten.Varje snitt tog ca 30 min att såga. snitt 7 var 236 cm från botten pro4.Snitt 8 var 242 cm från botten prov 5.Snitt 9 var 253 cm från botten prov 6.Snitt 10 var 259 cm från botten prov7. Snitt 11 var 265 cm Från botten prov8. Snitt 12 var 307 cm från botten.Snitt 13 var 313 cm från botten prov 9. Snitt 14 var 320 cm från botten prov 10.	6,5	JH			

Contractors' signatures and date		**SKB's signatures and date**	
Compiled by Jan Hultgren	Quality check for delivery	Delivery approved	Entered in SICADA